Simulated Docking of Oseltamivir with an Avian Influenza (A/H5N1) Neuraminidase Active Site

Jack K. Horner
P.O. Box 266
Los Alamos NM 87544 USA

Abstract

Given the lead-time currently required for vaccine production, a widespread administration of effective anti-influenza therapeutics is the only practical defense against a 1918-scale influenza pandemic after the pandemic begins. Neuraminidases are glycoproteins that facilitate the transmission of the influenza virus from cell to cell. The neuraminidase inhibitor osteltamivir is currently the most widely used anti-flu therapeutics. Oseltamivir was ineffective against the dominant H1N1 strains in the 2008 flu season and decreasingly effective against the dominant influenza H1N1 mutants in the US in the 2009 "Spring/Fall" pandemic. Several of the Influenza A/H5N1 mutants are genetically close to the 1918 pandemic strain. Here I provide a computational docking analysis of oseltamivir with the active site of the neuraminidase of an H5N1 strain. The computed inhibitor/receptor binding energy suggests that oseltamivir would not be effective against that strain. These results are consistent with the efficacy of oseltamivir observed in avian flu cases in humans.

Keywords: Influenza, H1N1, neuraminidase, oseltamivir

1.0 Introduction

The mortality rate in humans infected with Influenza A/H1N1 in the 1918 pandemic was ~50% ([2]). The 1918 mutant(s), unlike any genotype of H1N1 observed since, was easily transmitted among humans and killed ~10% of the world population within a single six-month period ([2]).

At present, no plausible public health regime could control an outbreak of a high-mortality-rate, highly infectious (HMR/HI) H1N1 mutant. The scale of human interaction required to sustain food and fuel distribution to large urban areas would render quarantine ineffective ([5]). Currently, the lead time for vaccine development and production is at least as long as the duration of the 1918 pandemic. A widespread administration of effective anti-influenza therapeutics is therefore the only practical defense against a 1918-scale event after the pandemic begins.

Neuraminidases are glycoproteins that facilitate the transmission of the influenza virus from cell to cell. The most widely used anti-influenza therapeutic, oseltamivir (Tamiflu™, [4]), was ineffective against the dominant H1N1 mutants in the 2008 flu season and was decreasingly effective against the dominant influenza mutant (Influenza A/H1N1) in the US in the 2009 "Spring/Fall" pandemic ([7]). Several of the Influenza A/H5N1 ("avian flu") mutants are genetically close to the 1918 pandemic strain. Avian flu in humans has not responded well to oseltamivir.

In the World Health Organization serotype-based influenza taxonomy, influenza type A has nine neuraminidase-related sero-subtypes, and these subtypes correspond at least roughly to differences in the active-site structures of the flu neuraminidases. The subtypes fall into two groups ([3]): group-1 contains the subtypes N1, N4, N5 and N8; group-2 contains the subtypes N2, N3, N6, N7 and N9.

Oseltamivir was designed to target the group-2 neuraminidases.

The available crystal structures of the group-1 N1, N4 and N8 neuraminidases ([1]) reveal that the active sites of these enzymes have a very different three-dimensional structure from that of group-2 enzymes. The differences lie in a loop of amino acids known as the "150-loop", which in the group-1 neuraminidases has a conformation that opens a cavity not present in the group-2 neuraminidases. The 150-loop contains an amino acid designated Asp 151; the side chain of this amino acid has a carboxylic acid that, in group-1 enzymes, points away from the active site as a result of the 'open' conformation of the 150-loop. The side chain of another active-site amino acid, Glu 119, also has a different conformation in group-1 enzymes compared with the group-2 neuraminidases (8]).

The Asp 151 and Glu 119 amino-acid side chains form critical interactions with neuraminidase inhibitors. For neuraminidase subtypes with the "open conformation" 150-loop, the side chains of these amino acids might not have the precise alignment required to bind inhibitors tightly ([8]). The active site of the 1918 strain has the 150-loop configuration.

The difference in the active-site conformations of the two groups of neuraminidases may also be caused by differences in amino acids that lie outside the active site. This means that an enzyme inhibitor for one target will not necessarily have the same activity against another with the same active-site amino acids and the same overall three-dimensional structure ([17]).

2.0 Method

The general objective of this study is straightforward: to computationally assess the binding energy of the active site of a crystallized Influenza A/H5N1 neuraminidase with oseltamivir. Unless otherwise noted, all processing described in this section was performed on a Dell Inspiron 545 with an Intel Core2 Quad CPU Q8200 (clocked @ 2.33 GHz) and 8.00 GB RAM, running under the *Windows Vista Home Premium (SP2)* operating environment.

Protein Data Bank (PDB) 2HU4 is a structural description of a crystallized neuraminidase of an H5N1 neuraminidase, bound to oseltamivir. 2HU4 consists of 8 identical chains, designated Chains A-H.

2HU4 was downloaded from PDB ([6]) on 31 January 2011. The ligand portion of 2HU4 was extracted using Microsoft *Word.* The automated docking suite *AutoDock Tools* v 4.2 (ADT, [9]) was used to perform the docking of oseltamivir to the receptor. More specifically, in ADT, approximately following the rubric documented in [12]

-- Chains B-H, and the water in Chain A, of 2HU4 were deleted

-- the ligand (oseltamivir) and Chain A's active-site was extracted (2HU4 identifies the active site of Chain A as 13 amides: ARG118, GLU119, ASP151, ARG152, TRP178, SER246, GLU276, GLU277, ARG292, TYR347, ARG371, and TYR406.)

-- the hydrogens, charges, and torsions in the ligand and active site were adjusted using ADT default recommendations, and finally, the ligand, assumed to be flexible wherever that assumption is physically possible, was auto-docked to the active site, assumed to be rigid, using the Lamarckian genetic algorithm implemented in ADT.

The ADT parameters for the docking are shown in Figure 1. Most values are, or are a consequence of, ADT defaults.

```
autodock_parameter_version 4.2       # used by autodock to validate parameter set
outlev 1                             # diagnostic output level
intelec                              # calculate internal electrostatics
seed pid time                        # seeds for random generator
ligand_types C HD OA N               # atoms types in ligand
fld 2HU4_receptor.maps.fld           # grid_data_file
map 2HU4_receptor.C.map              # atom-specific affinity map
map 2HU4_receptor.HD.map             # atom-specific affinity map
map 2HU4_receptor.OA.map             # atom-specific affinity map
map 2HU4_receptor.N.map              # atom-specific affinity map
elecmap 2HU4_receptor.e.map          # electrostatics map
desolvmap 2HU4_receptor.d.map        # desolvation map
move 2HU4_Ligand.pdbqt               # small molecule
about 0.5292 81.1637 109.1143        # small molecule center
tran0 random                         # initial coordinates/A or random
axisangle0 random                    # initial orientation
dihe0 random                         # initial dihedrals (relative) or random
tstep 2.0                            # translation step/A
qstep 50.0                           # quaternion step/deg
dstep 50.0                           # torsion step/deg
torsdof 7                            # torsional degrees of freedom
rmstol 2.0                           # cluster_tolerance/A
extnrg 1000.0                        # external grid energy
e0max 0.0 10000                      # max initial energy; max number of retries
ga_pop_size 150                      # number of individuals in population
ga_num_evals 2500000                 # maximum number of energy evaluations
ga_num_generations 27000             # maximum number of generations
ga_elitism 1                         # number of top individuals to survive to next
generation
ga_mutation_rate 0.02                # rate of gene mutation
ga_crossover_rate 0.8                # rate of crossover
ga_window_size 10                    #
ga_cauchy_alpha 0.0                  # Alpha parameter of Cauchy distribution
ga_cauchy_beta 1.0                   # Beta parameter Cauchy distribution
set_ga                               # set the above parameters for GA or LGA
sw_max_its 300                       # iterations of Solis & Wets local search
sw_max_succ 4                        # consecutive successes before changing rho
sw_max_fail 4                        # consecutive failures before changing rho
sw_rho 1.0                           # size of local search space to sample
sw_lb_rho 0.01                       # lower bound on rho
ls_search_freq 0.06                  # probability of performing local search on
individual
set_psw1                             # set the above pseudo-Solis & Wets parameters
unbound_model bound                  # state of unbound ligand
ga_run 10                            # do this many hybrid GA-LS runs
analysis                             # perform a ranked cluster analysis
```

Figure 1. ADT parameters for the docking in this study

Interatomic distances between ligand and receptor in the computed form were compared to those in 2HU4.

3.0 Results

The interactive problem setup, which assumes familiarity with the general neuraminidase "landscape", took about 15 minutes in ADT; the docking proper, about 29 minutes on the platform described in Section 2.0 The platform's performance monitor suggested that the calculation was more or less uniformly distributed across the four processors at ~25% of peak per processor (with occasional bursts to 40% of peak), and required a constant 2.9 GB of

memory.

Figure 2 shows the oseltamivir/receptor energy and position summary produced by ADT. The estimated free energy of binding is ~ -8.5 kcal/mol; the estimated inhibition constant, ~599 nanoMolar at 298 K. All distances between receptor and ligand atoms in the computed ligand position lie within 7% of the distances of the corresponding atoms in 2HU4.

```
       LOWEST ENERGY DOCKED CONFORMATION from EACH CLUSTER
        ________________________________________________


Keeping original residue number (specified in the input PDBQ file) for outputting.

MODEL       10
USER    Run = 10
USER    Cluster Rank = 1
USER    Number of conformations in this cluster = 10
USER
USER    RMSD from reference structure       = 1.083 A
USER
USER    Estimated Free Energy of Binding    =   -8.49 kcal/mol  [=(1)+(2)+(3)-(4)]
USER    Estimated Inhibition Constant, Ki   =  598.99 nM (nanomolar)  [Temperature =
298.15 K]
USER
USER    (1) Final Intermolecular Energy     =  -10.58 kcal/mol
USER        vdW + Hbond + desolv Energy     =   -6.25 kcal/mol
USER        Electrostatic Energy            =   -4.33 kcal/mol
USER    (2) Final Total Internal Energy     =   -1.19 kcal/mol
USER    (3) Torsional Free Energy           =   +2.09 kcal/mol
USER    (4) Unbound System's Energy  [=(2)] =   -1.19 kcal/mol
USER
USER
USER
USER    DPF = 2hu4.dpf
USER    NEWDPF move    2HU4_Ligand.pdbqt
USER    NEWDPF about   0.529200 81.163696 109.114304
USER    NEWDPF tran0   0.598137 80.588296 109.027331
USER    NEWDPF axisangle0     -0.942812 -0.318402 -0.098616 -12.108044
USER    NEWDPF quaternion0    -0.099435 -0.033581 -0.010401 -0.994423
USER    NEWDPF dihe0   -132.97 178.74 -163.16 -74.49 -77.91 6.34 21.37
USER
USER                              x       y       z    vdW   Elec        q     RMS
ATOM      1  C2  G39 A 800      -1.828  80.459 110.166 +0.10 +0.08    +0.091  1.083
ATOM      2  C3  G39 A 800      -1.053  79.024 110.281 -0.32 +0.01    +0.050  1.083
ATOM      3  C4  G39 A 800       0.139  78.772 109.253 -0.19 -0.11    +0.209  1.083
ATOM      4  C5  G39 A 800       0.996  80.037 109.196 -0.15 -0.03    +0.143  1.083
ATOM      5  C6  G39 A 800       0.097  81.256 108.700 -0.14 +0.00    +0.147  1.083
ATOM      6  C7  G39 A 800      -1.218  81.494 109.394 -0.12 +0.03    +0.049  1.083
ATOM      7  O7  G39 A 800       0.965  82.478 108.693 -0.00 -0.13    -0.379  1.083
ATOM      8  C8  G39 A 800       1.066  83.449 107.573 -0.12 +0.04    +0.121  1.083
ATOM      9  C9  G39 A 800       0.655  82.959 106.157 -0.21 +0.00    +0.027  1.083
ATOM     10  C91 G39 A 800       1.669  82.075 105.411 -0.17 +0.00    +0.007  1.083
ATOM     11  C81 G39 A 800       0.247  84.645 108.019 -0.27 +0.02    +0.027  1.083
ATOM     12  C82 G39 A 800      -1.056  84.731 107.289 -0.48 +0.00    +0.007  1.083
ATOM     13  N5  G39 A 800       2.104  79.738 108.210 -0.06 -0.03    -0.352  1.083
ATOM     14  H5  G39 A 800       1.870  79.493 107.248 +0.08 +0.01    +0.163  1.083
ATOM     15  C10 G39 A 800       3.397  79.792 108.587 -0.27 +0.10    +0.214  1.083
ATOM     16  C11 G39 A 800       4.411  79.477 107.550 -0.29 +0.07    +0.117  1.083
ATOM     17  O10 G39 A 800       3.796  80.089 109.751 -0.60 -0.23    -0.274  1.083
ATOM     18  N4  G39 A 800       0.914  77.622 109.714 +0.05 +0.08    -0.073  1.083
ATOM     19  H42 G39 A 800       0.767  77.422 110.704 -0.41 -0.44    +0.274  1.083
ATOM     20  H41 G39 A 800       0.695  76.824 109.117 +0.04 -0.55    +0.274  1.083
ATOM     21  H43 G39 A 800       1.914  77.816 109.758 -0.29 -0.25    +0.274  1.083
```

```
ATOM     22  C1  G39 A 800      -3.098  80.703 110.809 -0.23 +0.34    +0.177  1.083
ATOM     23  O1B G39 A 800      -3.839  81.683 110.469 -1.57 -1.96    -0.648  1.083
ATOM     24  O1A G39 A 800      -3.463  79.919 111.732 -0.62 -1.38    -0.648  1.083
```

Figure 2. ADT's oseltamivir energy and position predictions.

Figure 3 is a rendering of the active-site/inhibitor configuration computed in this study.

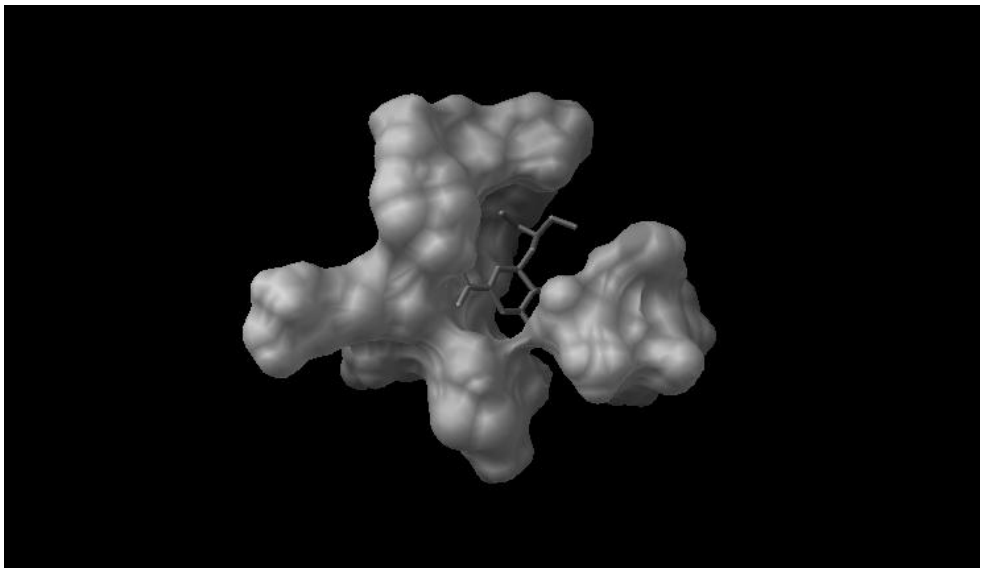

Figure 3. Rendering of oseltamivir computationally docked with the active site of Chain A of PDB 2HU4. The inhibitor is shown in stick form. Only the interior, inhibitor-containing region of the molecular surface of the active site can be compared to *in situ* data: the surface distal to the interior is a computational artifact, generated by the assumption that active site is detached from the rest of the receptor.

4.0 Discussion

The method described in Section 2.0 and the results of Section 3.0 motivate several observations:

1. The inhibition constant computed in this study (~599 nanoMolar at ~298 K) is comparable to the inhibition constant of oseltamivir/neuraminidase interactions that are not clinically effective ([11], [13]). This suggests that oseltamivir would not be effective against 2HU4.

2. All distances between receptor and ligand atoms in the computed ligand position lie within 7% of the distances of the corresponding atoms in 2HU4. (For electrostatic forces, a 7% distance difference would correspond to a (1.07^2 =) 14% difference in electrostatic force and potential energy. One could of course apply other statistics to the coordinate sets and provide a more comprehensive comparison of other forces/energies. Future work will address those issues.)

3. The docking study reported here assumes that the receptor is rigid. This assumption is appropriate for the binding energy computation for PDB 2HU4 per se. However, the calculation does not reflect what receptor "flexing" could contribute to the interaction of the ligand with native unliganded receptor. Future work will analyze the docking of the ligand with the native form.

4. The analysis described in Sections 2.0 and 3.0 assumes the neuraminidase is in a crystallized form. *In situ*, at physiologically normal temperatures (~310 K), the receptor is not in crystallized form. The ligand/receptor conformation *in situ*, therefore, may not be identical to their conformation in the crystallized form.

5. Minimum-energy search algorithms other than the Lamarckian genetic algorithm used in this work could be applied to this docking problem. Future work will use Monte Carlo/simulated annealing algorithms.

6. A variety of torsion and charge models could be applied to this problem, and future work will do so.

5.0 Acknowledgements

This work benefited from discussions with Tony Pawlicki. For any problems that remain, I am solely responsible.

6.0 References.

[1] Russell RJ et al. The structure of H5N1 avian neuraminidase suggests new opportunities for drug design. *Nature* 443 (6 September 2006), 45-49.

[2] Johnson NP and Mueller J. Updating the accounts: global mortality of the 1918-1920 "Spanish " influenza pandemic. *Bulletin of the History of Medicine* 76 (2002), 105-115.

[3] World Health Organization. A revision of the system of nomenclature for influenza viruses: a WHO memorandum. *Bulletin of the World Health Organization* 58 (1980), 585-591.

[4] Ward P et al. Oseltamivir (Tamiflu) and its potential for use in the event of an influenza pandemic. *Journal of Antimicrobial Chemotherapy* 55, supplement 1 (2005), i5-i21.

[5] Butler D. Avian flu special: The flu pandemic: were we ready? *Nature* 435 (26 May 2005), 400-402. doi: 10.1038/435400a.

[6] Russell RJ et al. The structure of H5N1 avian neuraminidase suggests new opportunities for drug design. *Nature* 443 (6 September 2006), 45-49. http://www.pdb.org/pdb/explore/explore.do?structureId=2HU4.

[7] US Centers for Disease Control. *Summary: Interim Recommendations for the Use of Influenza Antiviral Medications in the Setting of Oseltamivir Resistance among Circulating Influenza A (H1N1) Viruses, 2008-09 Influenza Season.* 19 December 2008. URL http://www.cdc.gov/flu/professionals/antivirals/summary.htm.

[8] Luo M. Structural biology: antiviral drugs fit for a purpose. *Nature* 443 (7 September 2006), 37-38. doi:10.1038/443037a, published online 6 September 2006.

[9] Morris GM, Goodsell DS, Huey R, Lindstrom W, Hart WE, Kurowski S, Halliday S, Belew R, and Olson AJ. *AutoDock* v4.2. http://autodock.scripps.edu/. 2010.

[10] Drug Bank. *Oseltamivir*. http://www.drugbank.ca/drugs/DB00198.

[11] Govorkova EA et al. Comparison of efficacies of RWJ-270201, zanamivir, and

oseltamivir against H5N1, H9N2, and other avian influenza viruses. *Antimicrobial Agents and Chemotherapy* 45 (2001), 2723-2732.

[12] Huey R and Morris GM. *Using AutoDock 4 with AutoDock Tools: A Tutorial.* 8 January 2008. http://autodock.scripps.edu/.

[13] Cheng Y and Prusoff WH. Relationship between the inhibition constant (K_i) and the concentration of inhibitor which causes 50 per cent inhibition (I_{50}) of an enzymatic reaction. *Biochemical Pharmacology* 22 (December 1973), 3099–3108. doi:10.1016/0006-2952(73)90196-2.